

Crystal Structure and Electrochemical Behavior of Li₂CuP: a Surprising Reversible Crystalline–Amorphous Transformation

O. Crosnier, C. Mounsey, P. Subramanya Herle, N. Taylor, and L. F. Nazar*

Department of Chemistry, University of Waterloo,
200 University Avenue West, Waterloo,
Ontario, N2L 3G1, Canada

Received July 11, 2003

Revised Manuscript Received November 6, 2003

Transition metal phosphides form an interesting class of solid state materials that are typically small band-gap semiconductors, with useful properties for luminescent devices and electronic components.¹ These compounds have also recently commanded attention as potentially new negative electrodes in lithium batteries. They act as good energy storage materials due to high uptake of lithium within the structure, giving rise to good gravimetric and volumetric capacities. They also exhibit unusual structural transformations initiated by redox processes. Several studies have demonstrated their complex electrochemical behavior during reaction with lithium, which varies according to the nature of the material. In the absence of a stable ternary Li–M–P phase, lithium insertion can cause phase decomposition similar to the case of other Group V compounds such as antimonides² – as demonstrated by CoP₃^{3,4} and CuP₂⁵ which both dissociate upon reduction to form Li₃P. Conversely, a metastable ternary phase can be formed, as demonstrated in the case of FeP₂ which reversibly uptakes 6 lithium to form amorphous Li₆FeP₂.⁶ More unusual is the electrochemically driven solid-state transformation between two crystalline phases, MnP₄ and Li₇MnP₄. This represents a pseudotopotactic insertion of lithium into MnP₄ accompanied by reversible cleavage/reformation of P–P bonds.⁷ Here, we report a new structural transformation within the class of phosphides, which demonstrates the reversible solid-state conversion between a crystalline phase (Li₂CuP) and a metastable binary disordered phase.

Li₂CuP was prepared by mixing stoichiometric amounts of metallic lithium (99.9%, Aldrich), metallic

Table 1. Li₂CuP Crystallographic Data (Space Group *P6₃/mmc*)^a

unit cell dimensions	<i>a</i> = 4.0481(3) Å <i>c</i> = 7.7086(13) Å		
<i>Z</i> , cell volume	2, 109.40(2) Å ³		
atomic positions	<i>x</i>	<i>y</i>	<i>z</i>
Cu	0	0	1/4
Li	1/3	2/3	0.5844(8)
P	1/3	2/3	1/4
selected distances (Å)	Cu–P (×3)	2.337(1)	
	Li–P (×3)	2.663(1)	
	Li–P (×1)	2.578(6)	
	Cu–Li (×6)	2.663(3)	
	Li–Li (×3)	2.675(4)	

^a R₁ = 2.1%; wR₂ = 4.4% (*I* > 2σ(*I*)).

copper (99.9%, Alfa Aesar), and red phosphorus (99%, Alfa Aesar), heated in an N₂ flow at 780 °C for 5 d in a stainless steel tube sealed under Ar, and quenched to room temperature. XRD patterns were collected on a Bruker D8 diffractometer equipped with two Goebel mirrors operating in parallel focusing geometry (Cu Kα radiation). Electrochemical experiments were performed in Swagelok-type cells and in an in situ cell with Be foil as the X-ray window, using metallic lithium as both counter and reference electrode. Electrodes were prepared by grinding the dark blue-black lustrous crystals of Li₂CuP in an inert atmosphere, mixing the compound with 20% carbon black (Super S), and compressing the mixture onto a Ni current collector. A 1 M solution of LiPF₆ dissolved in EC/DMC (1:1) was used as the electrolyte. The cells were assembled in an argon-filled glovebox and tested with a MacPile controller (Biologic S. A., Claix, France).

A suitable shiny black crystal with flat hexagonal morphology was isolated from the solid-state reaction mixture above and mounted on a Bruker APEX with graphite-monochromatized Mo Kα radiation (see Supporting Information for details). Structure refinement in the *P6₃/mmc* space group showed much better accuracy factors than the previously reported space group (*P3m1*) suggested by powder data.⁸ The cell parameters and atomic positions are given in Table 1. The structure of Li₂CuP is closely related to the well-known Li₃P phase (Figure 1),⁹ which is the same as the analogous nitride, β-Li₃N. The latter is a very good Li-ion conductor, although not quite as good as α-Li₃N, which displays among the highest Li-ion conductivity known (1 × 10^{−3} S/cm at 300 K).¹⁰ In Li₂CuP, layers of Li atoms reside between graphene-like sheets formed from a hexagonal arrangement of alternating Cu–P atoms. The Cu–P sheets (Figure 1a) are stacked along the *c*-axis in an AB arrangement (Figure 1b), similar to that of graphite. As shown in Figure 1c, the phosphorus atoms are surrounded by 3 copper atoms in the same plane, and by 8 lithium atoms; each of the latter forms a slightly distorted LiP₄ tetrahedron (Figure 1d). Unlike graphite,

* To whom correspondence should be addressed. E-mail: lfnazar@uwaterloo.ca.

(1) Aronsson, B.; Lundström, T.; Rundqvist, S. *Borides, Silicides and Phosphides: a Critical Review of their Preparation, Properties and Crystal Chemistry*; Wiley: New York, 1965.

(2) Fransson, L. M. L.; Vaughney, J. T.; Edstrom, K.; Thackeray, M. M. *J. Electrochem. Soc.* **2003**, *150*, A86. Thackeray, M. M.; Vaughney, J. T.; Johnson, C. S.; Kropf, A. J.; Benedek, R.; Fransson, L. M. L.; Edstrom, K. *J. Power Sources* **2003**, *113*, 124.

(3) Pralong, V.; Souza D. C. S.; Leung, T. K.; Nazar L. F. *Electrochem. Commun.* **2002**, *4*, 516.

(4) Alcantara, R.; Tirado, J. L.; Jumas, J. C.; Monconduit, L.; Olivier-Fourcade, J. *J. Power Sources* **2002**, *109*, 308.

(5) Wang, K.; Yang, J.; Xie, J.; Wang, B.; Wen, Z. *Electrochem. Commun.* **2003**, *5*, 480.

(6) Silva, D. C. C.; Crosnier, O.; Ouvrard, G.; Greedan, J.; Sefat-Sefat, A.; Nazar L. F. *Electrochem. Solid State Lett.* **2003**, *6*, A162.

(7) Souza, D. C. S.; Pralong, V.; Jacobson, A. J.; Nazar, L. F. *Science* **2002**, *296*, 2012.

(8) Schlenger, H.; Jacobs, H.; Juza, R. *Z. Anorg. Allg. Chem.* **1971**, *385*, 177.

(9) Brauer, G.; Zintl, E. *Z. Physik. Chem.* **1937**, *B37*, 323.

(10) Lapp, T.; Skaarup, S.; Hooper, A. *Solid State Ionics* **1983**, *11*, 97.

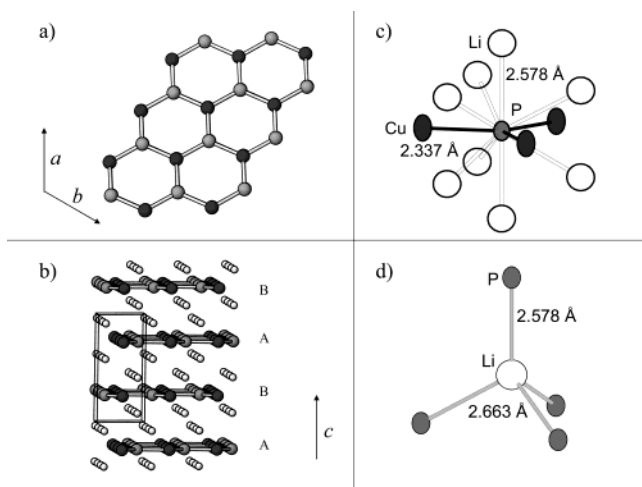


Figure 1. (a) Hexagonal arrangement of Cu/P atoms in the (1120 plane); (b) crystallographic structure of Li_2CuP ; (c) P atom environment; (d) Li atom environment. White, black, and gray atoms correspond to lithium, copper, and phosphorus, respectively. Atoms are drawn as 99% probability ellipsoids for (c) and (d).

there is strong covalent bonding of the lithium atoms to the layers that lie above and below the lithium sites. Li_2CuP can also be described as a copper-substituted form of $\alpha\text{-Li}_3\text{P}$, $\text{Li}_{3-x}\text{Cu}_x\text{P}$ ($x = 1$).¹¹

The voltage/composition curve (CCV) of Li_2CuP is shown in Figure 2a, for the first charge–discharge–charge process. On oxidation (charge), lithium is almost fully extracted from the structure to give a nominal composition of $\text{Li}_{0.25}\text{CuP}$, and is reversibly reinserted on reduction (discharge). The subsequent oxidation follows the first although some irreversibility occurs. The reversible lithium capacity corresponds to a specific gravimetric capacity of 430 mAh/g, greater than that of graphite (370 mAh/g);¹² its volumetric capacity is almost double that of graphite (1410 vs 830 mAh/cc) due to its higher density (3.28 g/cm³).

To better understand the processes that occur as a result of solid-state redox chemistry, we carried out studies using the galvanostatic intermittent titration technique (GITT)¹³ coupled with in-situ XRD experiments. The GITT experiments reveal that lithium extraction occurs in two distinct steps. First, a small plateau at 1.20 V vs Li^+/Li is associated with a complex phase transformation in the range between Li_2CuP and the composition $\text{Li}_{1.75}\text{CuP}$. Although the CCV suggests that a single phase is formed here, the OCV indicates possible solid solution behavior in this regime which merits further study. Upon further oxidation ($x(\text{Li}) < 1.75$), up to 1.5 lithium atoms can be removed from the structure at ca. 1.32 V vs Li^+/Li , described by the second well-defined phase transition (plateau). Complete extraction of the 2 lithium atoms in the starting phase to give a de-lithiated copper phosphide of theoretical composition “CuP” cannot be attained, even under these

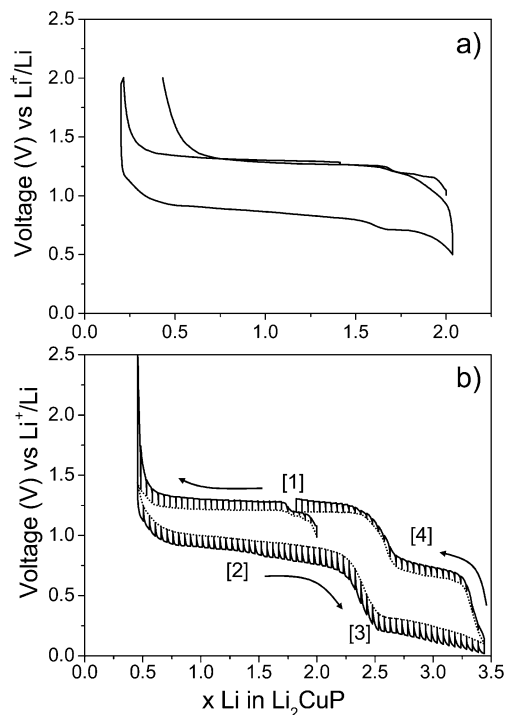


Figure 2. (a) Galvanostatic discharge between 0.5 and 2 V at a C/10 rate (1 Li every 10 h); (b) voltage vs composition electrochemical curve of Li_2CuP between 10 mV and 2.5 V vs Li^+/Li , performed using galvanostatic intermittent titration technique (GITT) with current pulses of 1 h equivalent to a C/20 rate followed by a 2-h relaxation period. Each spike represents the deviation of the voltage from its equilibrium value in the relaxation period following the current pulse. The voltage at the terminus of each spike thus corresponds to the OCV or near-equilibrium curve, shown by the dotted line.

quasi-equilibrium conditions.¹⁴ Although the final composition is close to that of the known material, LiCu_2P_2 ,¹⁵ the latter is unlikely to be formed (even in a disordered form; vide infra) as its Cu–P arrangement is very different from that in the starting phase, Li_2CuP . Upon reduction, lithium is reinserted into the structure in an apparent single-phase process down to 0.75 V. Extending the voltage window below 0.5 V revealed the presence of a phase transition at $x = 2.25$ leading to the $\text{Li}_{3.2}\text{CuP}$ composition, which is reversible on the subsequent charge cycle. A small contribution of the carbon added to the electrode to enhance its conductivity superimpose with the latter reactions at ca. 0.75 V vs Li^+/Li ; this contribution is subtracted to give the final lithium composition in the material at full discharge. The second oxidation leads to the starting composition Li_2CuP after lithium extraction at 0.75 V vs Li^+/Li .

The structural changes occurring in the material upon lithium cycling are shown in Figure 3. The data were collected by mounting an electrochemical cell directly in the X-ray diffractometer, and stopping the reaction at various stages of the deinsertion/reinsertion process after the relaxation step to acquire the X-ray pattern. A strong decrease in the XRD reflections is observed during lithium extraction, indicating that the oxidized

(11) Note that in the binary phase diagram only two copper phosphides exist (Cu_3P and CuP_2), and that no copper monophosphide “CuP” has been reported.

(12) Huggins, R. A. *Solid State Ionics* **2002**, *152*, 61.

(13) The GITT method employs a short current pulse followed by an open-circuit (OCV) step that permits the system to relax to equilibrium voltage before the subsequent step is applied.

(14) The fact that less lithium is removed from the structure than in the galvanostatic experiment is possibly due to a contact issue in this particular cell. Sampling of many electrochemical cells (>50) showed that consistently an average composition of $\text{Li}_{0.25}\text{CuP}$ was reached on oxidation.

(15) Schlenger, H.; Jabobs, H. *Acta Crystallogr.* **1972**, *B28*, 327.

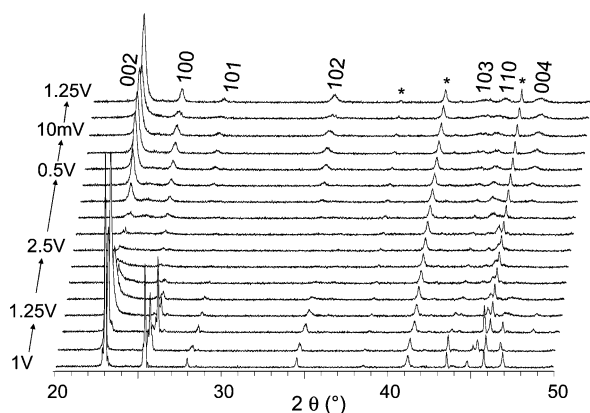


Figure 3. In situ XRD patterns of the Li_2CuP electrode recorded at different voltages upon cycling. The asterisks correspond to the cell hardware. The hkl indexes are shown on the top of the patterns.

phase is very disordered. The first complex transition that occurs between 1 and 1.25 V (equivalent to the removal of 0.25 Li) corresponds to region [1] observed in the electrochemical curve in Figure 2. It induces a small shift of the observed reflections as well as the appearance of additional weak peaks. The electrochemical deinsertion process is completely reversible in this regime ($2 < x < 1.75$; not shown). The pattern at the composition $\text{Li}_{1.75}\text{CuP}$ can be indexed in a hexagonal cell (same space group) with unit cell parameters $a = 7.9401 \text{ \AA}$; $c = 7.7484 \text{ \AA}$ close to that of pristine Li_2CuP ($a = 4.0481 \text{ \AA}$; $c = 7.7086 \text{ \AA}$). The new cell is related to the starting material by a doubling of the a axis, which accounts for the appearance of the additional peaks in the pattern.¹⁶ The changes compared to Li_2CuP are relatively small: they represent a negligible 0.04 \AA expansion along the c -axis and a 0.15 \AA contraction in the $(11\bar{2}0)$ plane. At the end of the oxidation at 2.5 V, very weak features representing a small amount of unreacted material remain in the pattern. A single new reflection arises at $2\theta = 45.8^\circ$ (d -spacing = 1.98 \AA), which was also the only feature observed in ex situ XRD experiments on samples removed from the cell at full oxidation. To understand its origin, X-ray absorption spectroscopy experiments are underway to determine the changes in the local environment of the CuP framework.

Most surprising is that recrystallization occurs during reduction. Progressive insertion of Li into the disordered "single peak" material initiates nucleation of the starting phase, indicated by the regrowth of the original diffraction pattern intensity in the voltage range to 0.5 V (region [2], Figure 2). Upon further Li insertion (to 10 mV, region [3], Figure 2) and extraction back to the starting composition Li_2CuP (region [4]), a diffraction pattern similar to that of the starting material is obtained, albeit with broadened lines. Some changes in relative intensities occur, especially among the first three diffractions peaks, which reflect changes in the coherence length along one or more of the crystal

directions. The behavior reported here is very different from that exhibited by the related nitride compositions ($\text{Li}_{3-x}\text{Co}_x\text{N}^{17}$ and $\text{Li}_{2.7}\text{Fe}_{0.3}\text{N}^{18}$) that become amorphous upon delithiation and remain in this state on subsequent cycling. In the phosphide, the Cu–P framework structure that is reformed at the end of the reduction is maintained during the second oxidation when the starting composition Li_2CuP is reached.

Oxidation–reduction involves the cleavage of Li–P bonds and their reformation on reduction. This is similar to graphite where Li–C bonding is established and disrupted on intercalation/deintercalation. In graphite, however, the insignificant structural changes exhibited on cycling demonstrate that the Li_2CuP framework is more susceptible to redox processes than is the robust carbon–carbon framework. Pertinent is the fact that both LiC_6 and graphite exist as thermodynamically stable phases, whereas a layered-phase copper phosphide "CuP" isostructural to Li_2CuP is not known. Differences in the band structure between graphite and Li_2CuP are responsible. Preliminary LMTO calculations for Li_2CuP show that the majority of the (filled) Cu d-bands are narrow and lie well below the Fermi level, indicating these d-orbitals do not participate in the redox process.¹⁹ The uppermost band in the DOS that lies just below the Fermi level, from which electrons are removed during oxidation, includes both Cu and P bonding states (not shown). Along with cleavage of the Li–P bonds, extraction of electron density from this band will affect the Cu–P bonding in the hexagonal framework (Figure 1a), and is undoubtedly responsible for the observed increase in structural disorder on oxidation. Nonetheless, the structural relaxation is reversible on reduction when the Cu–P band is repopulated. Thus, a significant role in the electrochemical process is adopted by the phosphorus anions as observed for other phosphides such as MnP_4 ⁷ and CoP_3 ³. The behavior exhibited by Li_2CuP shows that the facile covalent bond rearrangement in phosphides offers interesting perspectives in the search for new materials for lithium-ion batteries.

Acknowledgment. L.F.N. thanks NSERC for funding this work. We gratefully acknowledge Prof. Kleinke's loan of the software for the LMTO calculations, and for his capable assistance.

Supporting Information Available: Single crystal structure study (PDF) and crystallographic information file (CIF) for the subject material. This material is available free of charge via the Internet at <http://pubs.acs.org>.

CM034619M

(17) Shodai, T.; Okada, S.; Tobishima, S.; Yamaki, J. *Solid State Ionics* **1996**, *86*, 785. Nishijima M.; Kagohashi, T.; Imanishi H.; Takeda, Y.; Yamamoto, O.; Kondo, S. *Solid State Ionics* **2000**, *130*, 61.

(18) Rowsell, J. L. C.; Pralong, V.; Nazar, L. F. *J. Am. Chem. Soc.* **2001**, *123*, 8598.

(19) The self-consistent tight-binding *first principles* LMTO calculations (LMTO = linear muffin tin orbitals) were carried out using the structural parameters obtained from the refinement Li_2CuP . In the LMTO approach (Andersen, O. K. *Phys. Rev. B* **1975**, *12*, 3060), the density functional theory is used with the local density approximation (LDA). The k space integration was performed by an improved tetrahedron method on a grid of 488 irreducible k points of the first Brillouin zone.

(16) Crosnier, O.; Herle, P. S.; Nazar, L. F. Manuscript in preparation.